2021 43rd Annual International Conference of the
IEEE Engineering in Medicine & Biology Society (EMBC)
Oct 31 - Nov 4, 2021. Virtual Conference

Measuring the Rate of Information Transfer in Point-Process Data: Application to Cardiovascular Interactions

Gorana Mijatovic[1], *Member, IEEE*, Yuri Antonacci[2] and Luca Faes[3], *Senior Member, IEEE*

***Abstract*— We present the implementation to cardiovascular variability of a method for the information-theoretic estimation of the directed interactions between event-based data. The method allows to compute the transfer entropy rate (TER) from a source to a target point process in continuous time, thus overcoming the severe limitations associated with time discretization of event-based processes. In this work, the method is evaluated on coupled cardiovascular point processes representing the heartbeat dynamics and the related peripheral pulsation, first using a physiologically-based simulation model and then studying real point-process data from healthy subjects monitored at rest and during postural stress. Our results document the ability of TER to detect direction and strength of the interactions between cardiovascular processes, also highlighting physiologically plausible interaction mechanisms.**

I. Introduction

The transfer entropy (TE) is a well-known measure quantifying the directed information flow between stochastic processes [1]. It is widely used in many domains of science and engineering, including neuroscience where it is commonly employed to assess directional interactions between neurophysiological signals [2]; in cardiovascular variability analysis, TE has been used successfully to assess the direction and strength of the interactions between heart period, arterial pressure and respiration variability and to investigate the underlying physiological mechanisms [3], [4].

The TE has been originally defined and is typically computed for discrete-time processes, i.e. processes defined at discrete time instants which represent the sampling rate of continuous-time signals or the rate of a physiological oscillator (e.g., the cardiac pacemaker). In discrete time, the definition of TE is well-established and a number of practical approaches exist to provide data-efficient estimates [2], [4]. The definition of TE for continuous-valued processes, i.e. processes defined at each time instant with arbitrarily small resolution, is much more cumbersome. Recent theoretical work has defined a formalism to express the TE accumulated in continuous time over finite time intervals, deriving the expression of the corresponding TE rate (TER) [5]. Such work also highlighted the simplified form assumed by TER in the particular case of point processes, and was followed very recently by the formulation of an accurate non-parametric estimator of the TER for this class of processes [6].

Research supported by the Ministry of Education, Science and Technological Development of Serbia, project no. 451-03-68/2020- 14/200156, and by the Italian MIUR, project PRIN 2017 (PRJ-0167).

[1]G. M. is with the Faculty of Technical Sciences, University of Novi Sad, Novi Sad, Serbia email: gorana86@uns.ac.rs; Y.A.[2] is with the Dept. of Physics and Chemistry, University of Palermo, Italy; L.F.[3] is with the Dept. of Engineering, University of Palermo, Italy.

The work above has great practical relevance, as it opens the way for a reliable non-parametric, continuous-time estimation of the information transfer for event-based processes; previous efforts have mostly relied on parametric approaches [7], which have low flexibility, or on time discretization [8], which suffers from issues of bias and data requirement. We have recently implemented the formalism for the study of neural spike trains [9], and in this study we use it to assess the rate of information transfer between cardiovascular point processes. Specifically, we focus on cardiovascular interactions assessed between the cardiac pacemaker, studied by the heartbeat timings measured from the ECG, and the times of arrival to the body periphery of the sphygmic wave, measured through finger photoplethysmography. These interactions, which reflect the physiological mechanisms modulating the arterial pressure and the contractility of the ventricles and of the arteries [10], [11], are investigated in a simulated point process model of coupled heart rate and pulse rate variability and in real point process series measured from healthy subjects at rest and during postural stress.

II. Methods

A. Transfer Entropy Rate of Bivariate Point Processes

Given two possibly coupled systems whose evolution over time is mapped by the stationary stochastic processes X and Y, the directed transfer of information from Y to X is commonly assessed by the transfer entropy (TE) defined as $T_{Y\to X} = I(X_t; Y_t^- | X_t^-)$, where X_t denotes the present state of X, X_t^- and Y_t^- denote the past history of X and Y, and $I(\cdot;\cdot|\cdot)$ denotes conditional mutual information. The TE is well-established and widely used in discrete time, i.e. for processes defined at discrete time instants $t_n, n \in \mathbb{Z}$. On the other hand, its formulation in continuous time, i.e. for processes defined at each time instant $t \in \mathbb{R}$, relies on recent theoretical work [5] which evidenced the importance of defining a TE rate (TER) to ensure convergence of the measure. Specifically, the continuous-time TER from a source process Y to a target process X is defined as: [5]

$$\dot{T}_{Y\to X} = \frac{d}{dt}\mathbb{E}[\mathcal{T}_{Y\to X}^{[t_0,t]}(x_{[s,t]}, y_{[s,t)})], \tag{1}$$

where $\mathcal{T}_{Y\to X}^{[t_0,t]}(x_{[s,t]}, y_{[s,t)})$ is the so-called pathwise transfer entropy which represents the accumulated predictive capacity transferred from Y to X on the interval $[t_0, t]$ considering the path realizations $x_{[s,t]}$ and $y_{[s,t)}$ with $s \le t_0 < t$. The important work [5] derived also a formulation of the TER valid for point processes, i.e. processes described entirely by the times of occurrence of non-overlapping events, or spikes.

Given two point processes $X = \{x_i\}$ and $Y = \{y_j\}$, where x_i and y_j are the times of the i^{th} event in X and of the j^{th} event in Y, the TER is defined as: [5], [6]

$$\dot{T}_{Y\to X} = \overline{\lambda}_X \mathbb{E}_{p_x}\left[\ln \frac{\lambda_{X,x_i|X^-_{x_i},Y^-_{x_i}}}{\lambda_{X,x_i|X^-_{x_i}}}\right], \tag{2}$$

where $\overline{\lambda}_X = N_X/T$ is the average event rate of X, with N_X the number of target events and T the duration of the period analyzed. In Eq. (2), $\lambda_{X,x_i|X^-_{x_i}}$ and $\lambda_{X,x_i|X^-_{x_i},Y^-_{y_i}}$ are the instantaneous event rates of the target process X evaluated at the time of its i^{th} event x_i, conditioned respectively on the history of X and on the histories of both X and Y; the unconditioned instantaneous event rate of the process X, evaluated at the arbitrary time u, is $\lambda_{X,u} = \lim_{\Delta u\to 0} p_u\big(N_{X,u+\Delta u} - N_{X,u} = 1\big)/\Delta u$. At this point it is worth noting that, while the probability p_u is defined at any time point $u \in \mathbb{R}$, the expectation in (2) is taken over the probability p_x of observing a quantity at the time of target events x_i, $i = 1, \ldots, N_X$ [6]. This important distinction allows, after expressing the conditional event rates in terms of p_u, making a Bayes inversion and noting that $\lim_{\Delta u\to 0} p_u(\cdot|N_{X,u+\Delta u} - N_{X,u} = 1\big) = p_x(\cdot)$, to reformulate the expression of the TER as: [6]

$$\dot{T}_{Y\to X} = \overline{\lambda}_X \mathbb{E}_{p_x}\left[\ln\left(\frac{p_x(X^-_{x_i},Y^-_{x_i})}{p_u(X^-_{x_i},Y^-_{x_i})}\cdot\frac{p_u(X^-_{x_i})}{p_x(X^-_{x_i})}\right)\right], \tag{3}$$

showing that the TER depends on probabilities of the process histories $X^-_{x_i}$ and $Y^-_{x_i}$, evaluated at target events and at arbitrary time points (respectively, p_x and p_u), whose statistical average is taken only at target events (i.e., over p_x).

Eq. (3) provides the basis for estimating the TER in continuous time evaluating quantities at target events and representing histories by inter-event intervals. The estimation strategy followed here relies on creating history embeddings for the history of the target process and for the joint history of target and driver processes, followed by utilization of the k-Nearest-Neighbour (kNN) estimator to evaluate the four entropy terms resulting from (3) [6], [9]. The history embedding of the target X referred to the event x_i is approximated taking l inter-event intervals, i.e. $X^-_{x_i} \approx X^l_{x_i}$, where the k^{th} element of $X^l_{x_i}$ is the inter-event interval $x_{i-k+1} - x_{i-k}$. The history embedding of the driver Y referred to x_i is approximated as $Y^-_{x_i} \approx Y^l_{x_i} = [x_i - y_p, Y^{l-1}_{y_p}]$, where y_p is the most recent driver event preceding x_i. These history embeddings are then used in (3), which is expressed in terms of entropies to yield the TER estimate:

$$\begin{aligned}\hat{\dot{T}}_{Y\to X} = \overline{\lambda}_X[&\hat{H}_{p_u}(X^l_{x_i},Y^l_{x_i}) - \hat{H}_{p_x}(X^l_{x_i},Y^l_{x_i})\\ &+ \hat{H}_{p_x}(X^l_{x_i}) - \hat{H}_{p_u}(X^l_{x_i})]\end{aligned} \tag{4}$$

where $\hat{H}_{p_x}(\cdot)$ and $\hat{H}_{p_u}(\cdot)$ refer to 'standard' differential entropy estimate where expectation is taken over the same probability distribution for which the log-likelihood is estimated, and to 'cross-entropy' estimate where the two distributions differ [6]. Each entropy term of (4) is estimated using the kNN estimator (e.g., [2], [4]) with parameter k indicating the number of points used for neighbor search. Here, points are realizations of the history embeddings of dimension l or $2l$ specified in (4), and the search for neighbors is performed within the set of realizations taken at target events in the case of 'standard' entropy estimation, and within a set of realizations observed at arbitrary (randomly sampled) time points in the case of 'cross-entropy' estimation. The estimation algorithm, which is described in detail in refs. [6], [9], proceeds performing neighbor searches and range searches optimized to estimate together the four entropy terms in (4), in order to achieve compensation of the bias brought by the individual terms to the overall TER estimate.

III. Simulation Study

The proposed method for continuous-time TER estimation is evaluated on simulations of coupled point processes modeling the heartbeat events and the arrival times of the sphygmic wave in the body periphery. The process X, simulating the heartbeat times, is generated as a point process following the history-dependent inverse Gaussian (HDIG) model proposed in [12]. According to this model, given any R-wave event x_i, the waiting time until the next event, i.e. the i^{th} R-R interval w_i, is assumed to be drawn from the following probability density function:

$$p(w_i, X^p_{x_i}, \theta, \lambda) = \sqrt{\frac{\lambda}{2\pi w_i^3}}\cdot e^{\dfrac{-\lambda\big(w_i - \mu(X^p_{x_i},\theta)\big)^2}{2\mu(X^p_{x_i},\theta)^2 w_i}}, \tag{5}$$

where $\mu(X^p_{x_i},\theta)$ and λ are the mean and the scale parameter of the inverse Gaussian distribution. In the HDIG model, the mean is dependent on the history of the inter-event intervals up to the current event x_i, $X^p_{x_i} = [w_{i-1}, \cdots, w_{i-p}]$, according to the linear autoregressive (AR) model:

$$\mu(X^p_{x_i},\theta) = \theta_0 + \sum_{j=1}^{p}\theta_j w_{i-j}. \tag{6}$$

This model represents, through the parameter vector $\theta = (\theta_0, \theta_1, \cdots, \theta_p)$, the dependence of the R-R interval length on the history of the process, accounting for autonomic influences on heart rate variability [13]. In our simulation, we assume that the R-R intervals exhibit lagged dependencies up to the order p = 5, and set the coefficients $\{\theta_1, \cdots, \theta_5\}$ to obtain oscillations of w_i within the very low frequency (VLF), low frequency (LF) and high frequency (HF) bands typical of heart rate variability [13]; this was achieved simulating for the AR model (6) a transfer function with two complex-conjugate poles with modulus $\rho_{LF} = 0.8$ and phases $\pm 2\pi\cdot 0.1$ rad, two other complex-conjugate poles with modulus $\rho_{HF} = 0.92$ and phases $\pm 2\pi\cdot 0.25$ rad, and a real pole with modulus $\rho_{VLF} = 0.6$ [14]. The mean and scale parameters of the inverse Gaussian distribution are $\theta_0 = 1$ s and $\lambda = 600$ s. The R-R intervals generated by a run of the simulation are reported in Fig. 1 together with their power spectral density evidencing VLF, LF and HF oscillations.

After generating the heartbeat point process X as described above, the point process Y simulating the systolic

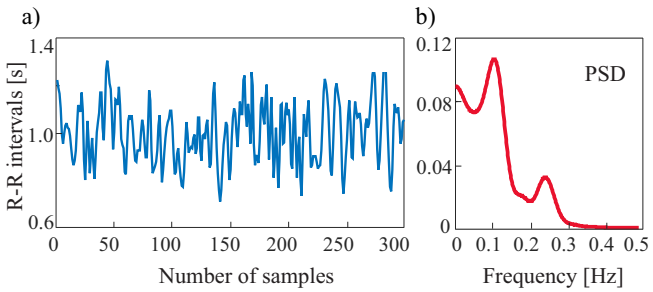

Fig. 1. (b) R-R intervals modeled as a history-dependent inverse Gaussian point process. (b) Power spectral density evidencing slow oscillations in the VLF band as well as LF and HF oscillations at ~ 0.1 Hz and ~ 0.25 Hz.

times is obtained generating its events as:

$$y_i = x_i + \tau + u_i, \tag{7}$$

where $\tau = 0.3$ s is the simulated mean pulse arrival time and u_i is a random time jitter modeling the part of the systolic time interval variability independent from heart rate variability. Here, values of u_i are drawn from the uniform distribution $\mathcal{U}(-\delta\tau, -\delta\tau+\delta w_i)$; with this choice, the parameter δ modulates the strength of the interaction from X to Y: when $\delta = 0$ we have $y_i = x_i + \tau$, corresponding to constant propagation time of the sphygmic wave; when $\delta = 1$ we have maximum uncertainty in the propagation times, which can take any value within the R-R interval ($y_i \in [x_i, x_i + w_i]$).

The analysis of TER is performed on 20 realizations of the simulation, each generated with $N_X = 300$ simulated heartbeats. For each pair of simulated spike trains, the TER is computed along the two directions of interaction using $k = 10$ neighbors. Results are presented showing the distribution across realizations of $\hat{\hat{T}}_{X\to Y}$ and $\hat{\hat{T}}_{Y\to X}$ for the analysis performed with length of the history embedding set at $l = 1$ (Fig. 2), and showing the distribution of $\hat{\hat{T}}_{X\to Y}$ for embedding lengths varying from $l = 1$ to $l = 5$ (Fig. 3). Moreover, in all simulations the statistical significance of the estimated TER values is assessed using surrogate data; pairs of surrogate event processes consist of the realization of the heartbeat $x = \{x_i\}$ (left untouched) and of a randomized realization of the systolic time process obtained adding to each simulated R-wave time a random propagation time ($y = \{y_i = x_i + u_i\}, u_i \in \mathcal{U}(0, w_i)$).

The simulation results show that the TER computed along the coupled direction $X \to Y$ is high and statistically significant for fully coupled processes ($\delta = 0$), and decreases progressively towards non-significant values as the jitter imposed to the propagation times increases (Fig. 2a); the TER values are non-significant for $\delta \geq 0.5$. Along the uncoupled direction $Y \to X$, the TER values are very low and almost never statistically significant for all values of δ (Fig. 2b). Increasing the length of the history embedding up to the memory imposed in the HDIG model ($l = p = 5$), the TER $X \to Y$ takes lower values but preserves the decreasing trend observed at increasing δ (Fig. 3a); interestingly, at increasing the uncoupling ($\delta \geq 0.3$) statistical significance of the TER $X \to Y$ was observed in a larger number of

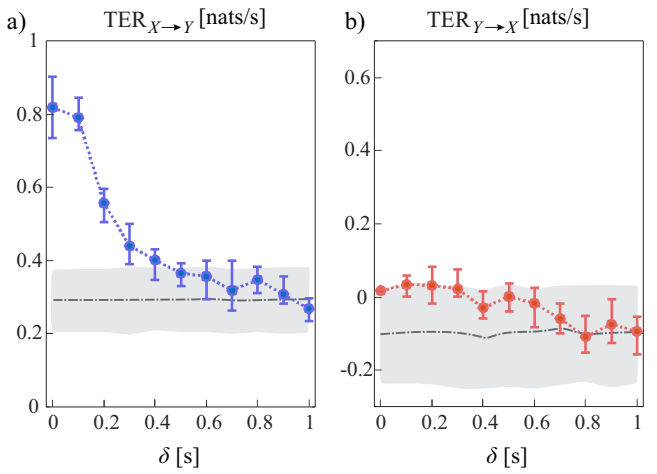

Fig. 2. Distribution (median and $25^{th} - 75^{th}$ percentiles over 20 realizations) of the TER estimated between the simulated point processes of the heartbeat times (X) and systolic times (Y), computed as a function of the de-coupling parameter δ. Gray shades denote the $5^{th} - 95^{th}$ percentiles of the distribution of TER computed over 100 surrogate pairs for each realization, averaged across realizations.

realizations when $l = 4, 5$ than for smaller lengths of the history embeddings (Fig. 3b).

IV. Application to Cardiovascular Variability

To provide a preliminary evaluation of the presented approach on real cardiovascular signals, we consider point-process data from a subgroup of 20 subjects randomly taken from the dataset of a previous study [15]. In the study, cardiovascular variability was assessed with subjects monitored in the resting supine position (REST) and during postural stress evoked by tilting the subjects in the upright position (TILT). Among the signals measured in [15], those relevant to the present study are the ECG and the finger photoplethysmographic arterial pressure signal, from which the heartbeat times (times of the R-wave in the ECG) and the times of occurrence of the systolic pressure (local maxima of the pressure signal) were measured on a beat-to-beat basis.

For each subject analyzed in the two conditions, series of 300 R-wave events (process X) and systolic time events (process Y) were considered for TER analysis. The analysis was performed with parameters $k = 10$ and $l = 2$. Our results document that the TER is substantial along the direction from R-wave to systolic times (Fig. 4a), while it is very low and often negative along the opposite direction from systolic to R-wave times (Fig. 4b). This confirms the expected unidirectional nature of this form of cardiovascular interaction. Moreover, the TER from R-wave to systolic times decreases significantly moving from the resting state to the head-up tilt condition (Fig. 4a). This result suggests that factors modulating the pulse rate variability independently of heart rate, possibly related to autonomic control of pre-ejection period and vessel contractility [11], are enhanced during postural stress. The result is in agreement with a previous study documenting lower agreement between heart rate and pulse rate variability during postural stress [16].

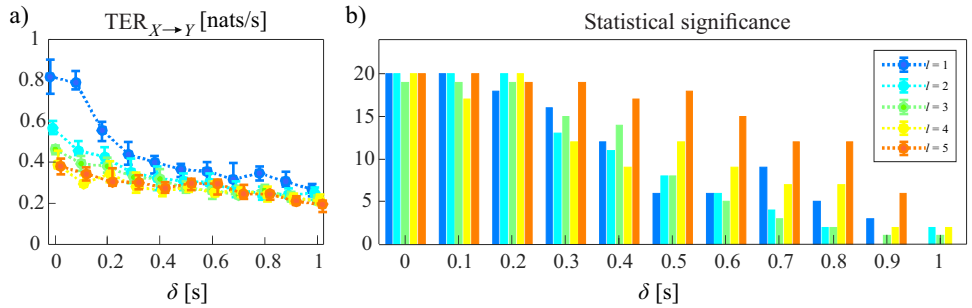

Fig. 3. a) Distribution (median and $25^{th} - 75^{th}$ percentiles over 20 realizations) of the TER estimated from the simulated heartbeat X to the simulated systolic times Yas a function of the de-coupling parameter δ, for different values of the history embedding length l; b) number of realizations for which the TER was detected as statistically significant for each combination of δ and l.

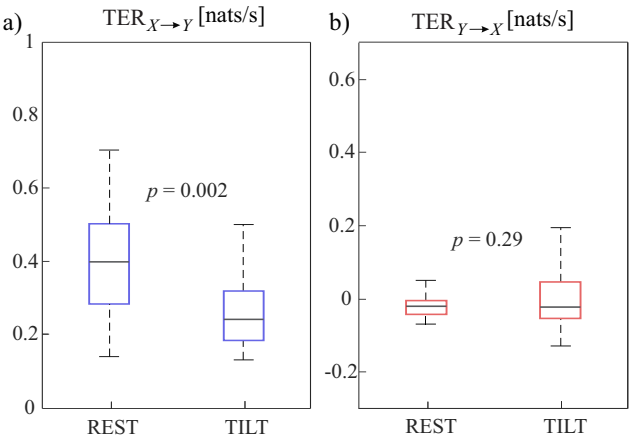

Fig. 4. Boxplot distribution of the TER estimated along the two directions of interaction between the heartbeat times X and the systolic times Y for 20 subjects studied at rest and during head-up tilt. p-values are relevant to a Wilcoxon signed-rank test for paired data comparing REST vs. TILT.

V. Conclusions

Cardiovascular interactions are commonly studied in the information-theoretic domain computing the TE between discrete-time processes mapping the heart period and systolic arterial pressure variability [3], [15].This study introduces an alternative approach based on the continuous-time estimation of the TE rate between point processes mapping the heartbeat and systolic time events. This approach, which explicitly considers the natural point-process structure of human heartbeats, can potentially uncover different mechanisms than those studied by the traditional TE analysis.

Future studies should explore the potential of this approach in more realistic simulation settings where physiological effects such as those related pre-ejection period and pulse transit time are considered [16], and in more challenging real data applications where the direction of interaction between point processes cannot be inferred a priori [9].

References

[1] T. Schreiber, "Measuring information transfer," *Phys. Rev. Lett.*, vol. 85, no. 2, p. 461, 2000.

[2] R. Vicente, M. Wibral, M. Lindner, and G. Pipa, "Transfer entropy—a model-free measure of effective connectivity for the neurosciences," *J. Comput. Neurosci.*, vol. 30, no. 1, pp. 45–67, 2011.

[3] L. Faes, D. Marinazzo, A. Montalto, and G. Nollo, "Lag-specific transfer entropy as a tool to assess cardiovascular and cardiorespiratory information transfer," *IEEE Trans. Biomed. Eng.*, vol. 61, no. 10, pp. 2556–2568, 2014.

[4] L. Faes, D. Kugiumtzis, G. Nollo, F. Jurysta, and D. Marinazzo, "Estimating the decomposition of predictive information in multivariate systems," *Phys. Rev. E*, vol. 91, no. 3, p. 032904, 2015.

[5] R. E. Spinney, M. Prokopenko, and J. T. Lizier, "Transfer entropy in continuous time, with applications to jump and neural spiking processes," *Phys. Rev. E*, vol. 95, no. 3, p. 032319, 2017.

[6] D. P. Shorten, R. E. Spinney, and J. T. Lizier, "Estimating transfer entropy in continuous time between neural spike trains or other event-based data," *PLoS computational biology*, vol. 17, no. 4, p. e1008054, 2021.

[7] G. Valenza, L. Faes, L. Citi, M. Orini, and R. Barbieri, "Instantaneous transfer entropy for the study of cardiovascular and cardiorespiratory nonstationary dynamics," *IEEE Trans. Biomed. Eng.*, vol. 65, no. 5, pp. 1077–1085, 2017.

[8] V. Pasquale, P. Massobrio, L. Bologna, M. Chiappalone, and S. Martinoia, "Self-organization and neuronal avalanches in networks of dissociated cortical neurons," *Neuroscience*, vol. 153, no. 4, pp. 1354–1369, 2008.

[9] G. Mijatovic, Y. Antonacci, T. L. Turukalo, L. Minati, and L. Faes, "An information-theoretic framework to measure the dynamic interaction between neural spike trains," *IEEE Transactions on Biomedical Engineering*, 2021.

[10] M. Okada, T. Matsuto, S. Satoh, S. Igarashi, M. Baba, O. Sugita, and M. Okada, "Role of pulse wave velocity for assessing autonomic nervous system activities in reference to heart rate variability," *Med. Inf.*, vol. 21, no. 1, pp. 81–90, 1996.

[11] G. S. Chan, P. M. Middleton, B. G. Celler, L. Wang, and N. H. Lovell, "Change in pulse transit time and pre-ejection period during head-up tilt-induced progressive central hypovolaemia," *J. Clin. Monitoring Comput.*, vol. 21, no. 5, pp. 283–293, 2007.

[12] R. Barbieri, E. C. Matten, A. A. Alabi, and E. N. Brown, "A point-process model of human heartbeat intervals: new definitions of heart rate and heart rate variability," *Am. J. Physiol.*, vol. 288, no. 1, pp. H424–H435, 2005.

[13] P. K. Stein, M. S. Bosner, R. E. Kleiger, and B. M. Conger, "Heart rate variability: a measure of cardiac autonomic tone," *Am. Heart J.*, vol. 127, no. 5, pp. 1376–1381, 1994.

[14] A. Beda, D. M. Simpson, and L. Faes, "Estimation of confidence limits for descriptive indexes derived from autoregressive analysis of time series: Methods and application to heart rate variability," *PloS One*, vol. 12, no. 10, p. e0183230, 2017.

[15] M. Javorka, J. Krohova, B. Czippelova, Z. Turianikova, Z. Lazarova, K. Javorka, and L. Faes, "Basic cardiovascular variability signals: mutual directed interactions explored in the information domain," *Phys. Meas.*, vol. 38, no. 5, p. 877, 2017.

[16] R. Pernice, M. Javorka, J. Krohova, B. Czippelova, Z. Turianikova, A. Busacca, and L. Faes, "Comparison of short-term heart rate variability indexes evaluated through electrocardiographic and continuous blood pressure monitoring," *Med. Biol. Eng. Comput.*, vol. 57, no. 6, pp. 1247–1263, 2019.